Jurnal Kejuruteraan 34(6) 2022: 1209-1214
https://doi.org/10.17576/jkukm-2022-34(6)-21

Physical Properties of Sintered Stainless Steel 17-4PH Micro-Part Processed by Micro-Powder Injection Molding

Al Basir*, Abu Bakar Sulong, Nashrah Hani Jamadon & Norhamidi Muhamad

Department of Mechanical and Manufacturing Engineering, Faculty of Engineering and Built Environment, Universiti Kebangsaan Malaysia, 43600 Bangi, Selangor, Malaysia

**Corresponding author: al.basir005@yahoo.com*

Received 1 April 2022, Received in revised form 19 May 2022
Accepted 20 June 2022, Available online 30 November 2022

ABSTRACT

Micro-powder injection molding (μPIM) is a modification of powder injection molding (PIM) process and a globally recognized manufacturing process route that can be used largely to produce sophisticated micro-sized components using a wide range of metals and ceramics. The demand of μPIM process is currently increasing in various applications in telecommunication, electronics, aerospace, biomedical, and automotive industries. In this research work, sintering at three different temperatures between 1250 °C and 1350 °C at a heating rate of 10 °C/min with a dwelling period of 3 h on micro-injection molded and debound (solvent and thermal) micro-sized components of stainless steel 17-4PH (SS 17-4PH) was carried out. After the sintering operation, defect-free SS 17-4PH micro-specimens were achieved. The relative density, which is referred to as an important physical property of SS 17-4PH micro-parts, increased substantially from 95.3% to 97.5% when the sintering temperature was enhanced from 1250 °C to 1350 °C. The maximum shrinkage of 12.9% was observed in micro-sized specimens at the sintering temperature of 1350 °C. After the completion of sintering process, the findings revealed that SS 17-4PH micro-parts can be produced successfully on the grounds of μPIM process employing the SS 17-4PH feedstock with powder loading of 69 vol.%.

Keywords: Micro-powder injection molding; SS 17-4PH; sintering; physical properties

INTRODUCTION

As pertaining to powder metallurgy, the powder injection molding (PIM) is a prominent fabrication method and a financially sustainable approach for producing complicated, near net shape macro-sized components (Dehghan-Manshadi et al. 2018; Basir et al. 2020a). Over the past several decades, the inclination of the world market towards the production of micro-components to employ in different engineering and technological applications has accelerated the evolvement of micro-powder injection molding (μPIM) from PIM. Both the PIM and μPIM processes, which are involved in fabricating macro and micro-sized parts, respectively, have come up with various advantages such as cost-effective production process, the broad spectrum of materials options, the opportunity of mass production, excellent design and surface finish, marginal materials loss, excellent mechanical properties, and high performance (Attia et al. 2014; Dehghan-Manshadi et al. 2018; Emeka et al. 2017; Liu et al. 2018; Moghadam et al. 2021; Ouyang et al. 2020; Piotter et al. 2011; Trad et al. 2020; Wang et al. 2014). While the macro-components produced from the PIM technique have the average size of nearly a few centimeters, the micro-sized parts fabricated through the μPIM method have the extrinsic dimension of around a few millimeters. When it comes to micro-structured components, the external dimension can reach to a few centimeters. The weight is the major concern for micro-weight components, and it requires to be less than 1 g. The dimensional consideration is an insignificant factor for micro-precision components that possess the tolerances in micro-scale (Huang 2006; Meng 2011; Tosello et al. 2010).

The development of precipitation-hardened martensitic stainless steel was carried out in the year of 1940 with the intention to eliminate the challenges of completely austenitic and martensitic stainless steels in terms of toughness, strength, high performance in elevated temperatures, and ductility (Hsiao et al. 2002; Smith 1993; Yoo et al. 2006). Among the steels, stainless steel 17-4PH (SS 17-4PH) is a widely known precipitation hardening steel and often designated as Grade 630. SS 17-4PH has got overarching priority in different applications because of having excellent features and properties such as very high strength, excellent resistance to pitting and corrosion, very high resistance to fatigue, excellent weldability, and viability (Emeka et al. 2017; Muñoz et al. 2006; Murr et al. 2012; Schade et al. 2009; Schade et al. 2008; Tian et al. 2017). Due to having a good number of specificities, the usage of SS 17-4PH in different applications has been increased over the years. Currently, SS 17-4PH is extensively using in aerospace

industries, defense industries, food processing plant, paper and pulp industries, oil refining equipment, and chemical industries (Gaona-Tiburcio et al. 2001; Kazior et al. 2013; Lo et al. 2009; Schade & Stears 2007; Viswanathan et al. 1989).

The machining process of SS 17-4PH is a complex task due to its high hardness, and in order to resolve this manufacturing complication, the PIM process has been taken into account as an alternative pathway for the fabrication of SS 17-4PH components. Several researches have already been conducted to fabricate macro-sized SS 17-4PH components implementing the PIM technique (Li et al. 2007; Sung et al. 2002; Ye et al. 2008; Zhang & German 1992). The demand of micro-sized components is increasing in the global market to use in different engineering applications. Therefore, in this study, the physical properties of sintered SS 17-4PH micro-parts produced through the µPIM process was investigated.

EXPERIMENTAL PROCEDURES

As a raw material, SS 17-4PH powder was supplied by Inframat Advanced Materials LLC, USA. The mean particle size and the pycnometer density of SS 17-4PH were obtained as 7.5 µm and 7.7435 g/cm^3, respectively, and were measured with Microtrac X100 and AccuPyc II 1340 Gas Displacement Pycnometry System, respectively. The scanning electron microscope (SEM) image of the 17-4PH powder is demonstrated in Figure 1. The X-ray diffraction (XRD) analysis of SS 17-4PH powder is shown in Figure 2. In connection with 17-4PH powder, as can be seen in Figure 2, the major elements are iron (Fe), chromium (Cr), and nickel (Ni). Usually, the presence of Cr as an alloying element upgrades the corrosion resistance property of SS 17-4PH. In this study, the binder system was comprised of palm stearin (PS) and low-density polyethylene (LDPE), respectively. The density of PS and LDPE were 0.891 and 0.91 g/cm^3, respectively, and were purchased from Sime Darby Kempas Sdn. Bhd. and Polyolefin Company (Singapore) Pte Ltd., respectively.

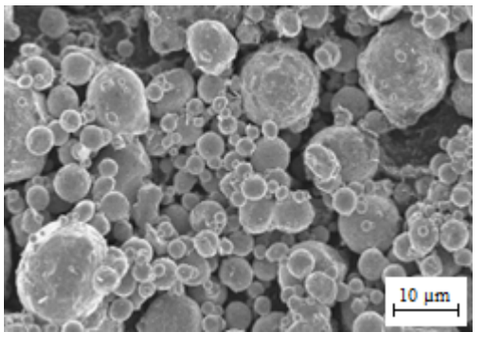

FIGURE 1. Morphology of SS 17-4PH powder

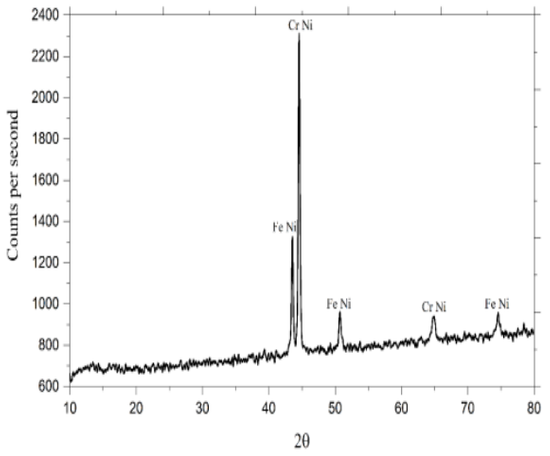

FIGURE 2. XRD analysis of SS 17-4PH

In order to prepare the SS 17-4PH feedstock, 69 vol.% of 17-4PH stainless steel was considered for mixing with PS and LDPE binders in a Brabender mixer (W50 EHT) maintaining the mixing temperature, time, and speed of 150 °C, 45 min, and 25 rpm, respectively, to keep the feedstock viscosity into an allowable level for micro-injection molding (Basir et al. 2020b; Basir et al. 2021). Semi-automatic DSM Xplore injection molding machine was used to produce SS 17-4PH micro-parts on the grounds of the previously studied parameters (Basir et al. 2020b) and is shown in Table 1. The dimensions of the micro-sized components of SS 17-4PH are schematically depicted in Figure 3.

The process of solvent extraction of the green SS 17-4PH micro-parts was carried out by employing MMM VentiCell 111 oven under previously investigated parameters (Basir et al. 2020b). With the intention to remove the PS binder, the green micro-sized SS 17-4PH samples were immersed in acetone for 40 min at the solvent debinding temperature of 70 °C. Afterwards, the thermal debinding was carried out on solvent debound SS 17-4PH micro-specimens at 550 °C for 2 h in argon environment using a tube furnace to eliminate the insoluble LDPE and remaining PS binders (Basir et al. 2021). The thermally debound micro-sized specimens of SS 17-4PH were heated from 550 °C to three different sintering temperatures between 1250 °C and 1350 °C at a heating rate of 10 °C /min for 3 h in the same argon environment. The density and the shrinkage percentage of the sintered samples were measured following MPIF standard 42 and MPIF standard 44, respectively (Fayyaz et al 2018).

TABLE 1. Parameters to fabricate micro-sized SS 17-4PH samples

Injection molding parameters	Operational process
Injection/compression/ holding pressure	10 bar
Mold temperature	65 °C
Melt temperature	180 °C
Injection/compression/ holding time	7 s

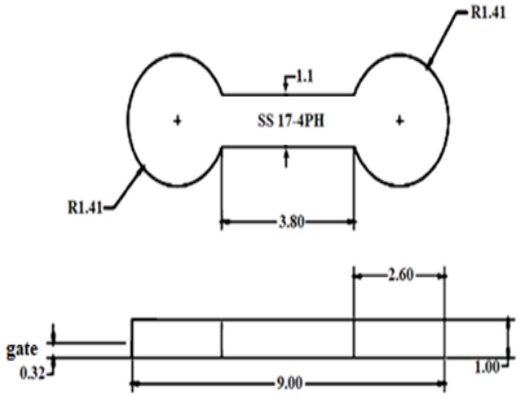

FIGURE 3. Dimensions of the 17-4PH stainless steel micro-sized component (mm)

RESULTS AND DISCUSSION

The field emission scanning electron microscope (FESEM) image of the SS 17-4PH feedstock is demonstrated in Figure 4. Based on Figure 4, the powder particles of 17-4PH were effectively covered with PS and LDPE binders. The green 17-4PH micro-sized component structure after the process of solvent debinding is depicted in Figure 5. Due to solvent debinding process, the PS binder was eliminated suitably from the SS 17-4PH micro-part. The FESEM image of the thermal debound SS 17-4PH micro-part is shown in Figure 6, which indicated that the insoluble LDPE and the remaining PS binder were mostly removed after the thermal debinding process. The open-pore structure that formed during the process of solvent extraction mainly helped to successfully remove the binder system during thermal debinding. Basically, after the thermal debinding process, the micro-components become very fragile and therefore requires to handle carefully for the next processing stage (Fayyaz et al. 2014).

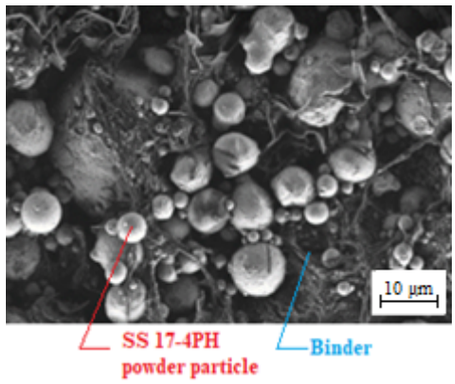

FIGURE 4. FESEM image of SS 17-4PH feedstock

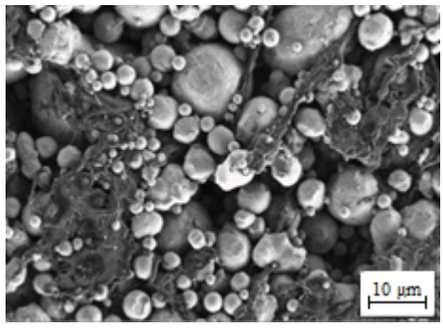

FIGURE 5. FESEM image of solvent debound SS 17-4PH micro-part

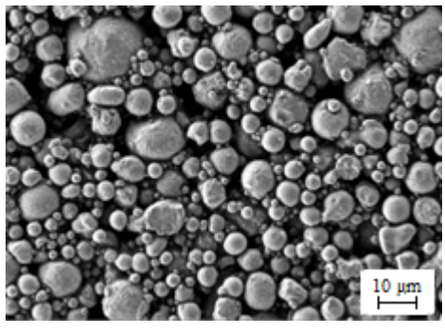

FIGURE 6. FESEM image of thermal debound SS 17-4PH micro-part

The photograph and the SEM image of the sintered SS 17-4PH micro-component are shown in Figure 7 and Figure 8, respectively. No defects were observed in the sintered component. Measuring the relative density is considered as an important factor in sintering due to the occurrence of eradication of pores as a consequence of the diffusion

of molecules and grain growth densification (German et al. 2013; Ramli et al. 2019). The relative densities of the 17-4PH stainless steel micro-sized parts sintered at three different temperatures between 1250 °C and 1350 °C is shown in Table 2. As can be seen in Table 2, the relative density of the samples increased from 95.3% to 97.2% with the increase of the sintering temperature from 1250 °C to 1300 °C. The further increase of the sintering temperature to 1350 °C gave a very little increase of the relative density to 97.5%. It is required for the PIM-based component to display relative density higher than 95%, and it is advisable to employ sintering temperature higher than 1250 °C during the fabrication of SS 17-4PH micro-parts (Heaney 2012).

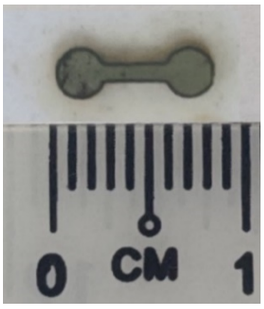

FIGURE 7. Photograph of sintered SS 17-4PH micro-part

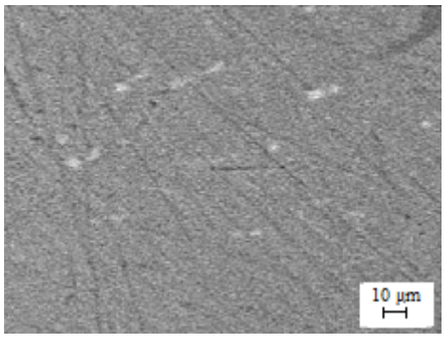

FIGURE 8. SEM image of sintered micro-part

TABLE 2. Relative densities of SS 17-4PH micro-parts

Sintering temperature (°C)	Relative density (%)
1250	95.3
1300	97.2
1350	97.5

Shrinkage is a common phenomenon in PIM and µPIM-based components (Basir et al. 2022; Foudzi et al. 2013; Imgrund et al. 2008). The occurrence of linear shrinkage in micro-sized SS 17-4PH components at sintering temperatures between 1250 °C-1350 °C with a holding period of 3 h is demonstrated in Figure 9. Based on Figure 9, an increase of shrinkage percentage from 9.3% to 12.9% was observed in SS 17-4PH micro-parts while temperature during sintering was enhanced from 1250 °C to 1350 °C. The range of shrinkage between 15% to 25% is often observed in µPIM-processed micro-parts (Heldele et al. 2006; Piotter et al. 2003).

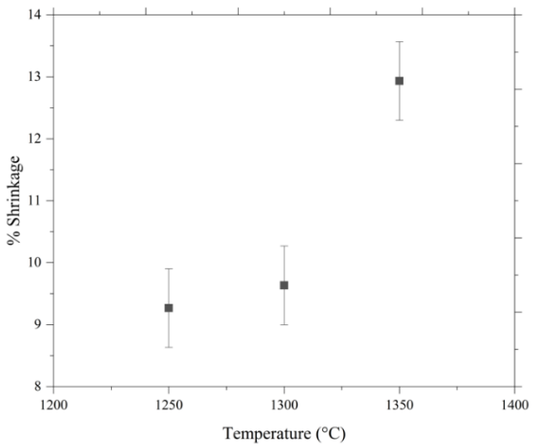

FIGURE 9. Shrinkages occurred in SS 17-4PH micro-parts

CONCLUSION

The aim of this study was to investigate the physical properties of micro-injection molded SS 17-4PH micro-parts. After the micro-injection molding process by applying the required parameters, the green SS 17-4PH micro-parts were subjected to solvent and thermal debinding processes where the binder system was removed successfully. The relative density of the micro-szed SS 17-4PH components was reached to more than 97% when the sintering temperature of 1300 °C or higher was applied. The sintered micro-components displayed maximum shrinkage level of 12.9% compared to the green components when sintering was carried out at 1350 °C. This research work will help to understand the sintering behavior of µPIM-processed SS 17-4PH micro-parts.

ACKNOWLEDGEMENT

The authors would like to thank Ministry of Higher Education Malaysia and Universiti Kebangsaan Malaysia for their financial support under the grant FRGS/1/2021/TK0/UKM/01/2 and DIP-2020-008.

DECLARATION OF COMPETING INTEREST

None

REFERENCES

Attia, U. M., Hauata, M., Walton, I., Annicchiarico, D. & Alcock, J. R. 2014. Creating movable interfaces by micro-powder injection moulding. *Journal of Materials Processing Technology* 214 (2): 295–303.

Basir, A., Sulong, A. B., Eshak, E., Mas'ood, N. N., Jamadon, N. H. & Muhamad, N. 2020a. Moldability of nano size zirconia for powder injection molding process by using PEG and PMMA binders. *Jurnal Kejuruteraan* 32 (2): 335–339.

Basir, A., Sulong, A. B., Jamadon, N. H. & Muhamad, N. 2020b. Bi-material micro-part of stainless steel and zirconia by two-component micro-powder injection molding: rheological properties and solvent debinding behavior. *Metals* 10 (5): 595.

Basir, A., Sulong, A. B., Jamadon, N. H. & Muhamad, N. 2021. Feedstock properties and debinding mechanism of yttria-stabilized zirconia/ stainless steel 17-4PH micro-components fabricated via two-component micro-powder injection molding process. *Ceramics International* 47 (14): 20476–20485.

Basir, A., Sulong, A. B., Jamadon, N. H. & Muhamad, N. 2022. Sintering behavior of bi-material micro-component of 17-4PH stainless steel and yttria-stabilized zirconia produced by two-component micro-powder injection molding process. *Materials* 15 (6): 2059.

Dehghan-Manshadi, A., StJohn, D., Dargusch, M., Chen, Y., Sun, J. F. & Qian, M. 2018. Metal injection moulding of non-spherical titanium powders: Processing, microstructure and mechanical properties. *Journal of Manufacturing Processes* 31: 416–423.

Emeka, U. B., Sulong, A. B., Muhamad, N., Sajuri, Z. & Salleh, F. 2017. Two component injection moulding of bi-material of stainless steel and yttria stabilized zirconia – green part. *Jurnal Kejuruteraan* 29 (1): 49–55.

Foudzi, F. M., Muhamad, N., Bakar Sulong, A. & Zakaria, H. 2013. Yttria stabilized zirconia formed by micro ceramic injection molding: Rheological properties and debinding effects on the sintered part. *Ceramics International* 39(3): 2665–2674.

Fayyaz, A., Muhamad, N. & Sulong, A. B. 2018. Microstructure and physical and mechanical properties of micro cemented carbide injection moulded components. *Powder Technology 326: 151–158.*

Fayyaz, A., Muhamad, N., Sulong, A. B., Rajabi, J. & Wong, Y. N. 2014. Fabrication of cemented tungsten carbide components by micro-powder injection moulding. *Journal of Materials Processing Technology 214(7): 1436–1444.*

German, R.M. 2013. Progress in titanium metal powder injection molding. *Materials* 6: 3641–3662.

Gaona-Tiburcio, C., Almeraya-Calderón, F., Martinez-Villafañe, A. & BautistaMargulis, R. 2001. Stress corrosion cracking behaviour of precipitation hardened stainless steels in high purity water environments. *Anti-Corrosion Methods and Materials* 48(1): 37–46.

Huang, C. K. 2006. Filling and wear behaviors of micro-molded parts made with nanomaterials. *European Polymer Journal* 42(9): 2174–2184.

Hsiao, C. N., Chiou, C. S. & Yang, J. R. 2002. Aging reactions in a 17-4 PH stainless steel. *Materials Chemistry and Physics* 74(2): 134–142.

Heldele, R., Rath, S., Merz, L., Butzbach, R., Hagelstein, M. & Haußelt, J. 2006. X-ray tomography of powder injection moulded micro parts using synchrotron radiation. *Nuclear Instruments and Methods in Physics Research Section B: Beam Interactions with Materials and Atoms* 246(1): 211–216.

Heaney, D. F. 2012. *Handbook of metal injection molding*. Cambridge, UK: Woodhead Publishing.

Imgrund, P., Rota, A. & Simchi, A. 2008. Microinjection moulding of 316L/17-4PH and 316L/Fe powders for fabrication of magnetic-nonmagnetic bimetals. *Journal of Materials Processing Technology* 200(1–3): 259–264.

Kazior, J., Szewczyk-Nykiel, A., Pieczonka, T., Hebda, M. & Nykiel, M. 2013. Properties of precipitation hardening 17-4 PH stainless steel manufactured by powder metallurgy technology. *Advanced Materials Research* 811: 87–92.

Li, Y., Li, L. & Khalil, K. A. 2007. Effect of powder loading on metal injection molding stainless steels. *Journal of Materials Processing Technology* 183(2–3): 432–439.

Liu, L., Gao, Y. Y., Qi, X. T. & Qi, M. X. 2018. Effects of wall slip on ZrO_2 rheological behavior in micro powder injection molding. *Ceramics International* 44(14): 16282–16294.

Lo, K. H., Shek, C. H. & Lai, J. K. L. 2009. Recent developments in stainless steels. *Materials Science and Engineering R* 65 (4–6): 39–104.

Muñoz, M. C., Gallego, S., Beltrán, J. I. & Cerdá, J. 2006. Adhesion at metal–ZrO_2 interfaces. *Surface Science Reports* 61(7): 303–344.

Murr, L. E., Martinez, E., Hernandez, J., Collins, S., Amato, K. N., Gaytan, S. M. & Shindo, P. W. 2012. Microstructures and properties of 17-4 PH stainless steel fabricated by selective laser melting. *Journal of Materials Research and Technology* 1(3): 167–177.

Moghadam, M. S., Fayyaz, A. & Ardestani, M. 2021. Fabrication of titanium components by low-pressure powder injection moulding using hydridedehydride titanium powder. *Powder Technology* 377: 70–79.

Meng, J., Loh, N. H., Fu, G., Tay, B. Y. & Tor, S. B. 2011. Micro powder injection moulding of alumina micro-channel part. Journal of the *European Ceramic Society* 31(6): 1049–1056.

Ouyang, M., Xu, L., Zhang, Q., Wang, C., Wang, C., Zhang, H. & Liu, X. 2020. Effects of jet milling on W–10 wt.%Cu composite powder for injection molding. *Journal of Materials Research and Technology* 9(4): 8535–8543.

Piotter, V., Bauer, W., Knitter, R., Mueller, M., Mueller, T. & Plewa, K. 2011. Powder injection moulding of metallic and ceramic micro parts. *Microsystem Technologies* 17(2): 251–263.

Piotter, V., Gietzelt, T. & Merz, L. 2003. Micro powder-injection moulding of metals and ceramics. *Sadhana* 28: 299–306.

Ramli, M.I., Sulong, A.B., Muhamad, N., Muchtar, A. & Zakaria, M.Y. 2019. Effect of sintering on the microstructure and mechanical properties of alloy titanium-wollastonite composite fabricated by powder injection moulding process. *Ceramics International* 45: 11648–11653.

Smith, W. F. 1993. *Structure and properties of engineering alloys*. McGraw-Hill.

Sung, H. J., Ha, T. K., Ahn, S. & Chang, Y. W. 2002. Powder injection molding of a 17-4 PH stainless steel and the effect of sintering temperature on its microstructure and mechanical properties. *Journal of Materials Processing Technology* 130–131: 321–327.

Schade, C., Schaberl, J. & Lawley, A. 2008. Stainless steel AISI grades for PM applications. *International Journal of Powder Metallurgy* 44(3): 57–67.

Schade, C. & Stears, P. 2007. Precipitation hardening PM stainless steel. *International Journal of Powder Metallurgy* 43(4): 51–59.

Schade, C. T., Murphy, T., Lawley, A. & Doherty, F. R. 2009. Development of a dual-phase precipitation-hardening PM stainless steel. *International Journal of Powder Metallurgy* 45(1): 38–46.

Trad, M. A. B., Demers, V., Côté, R., Sardarian, M. & Dufresne, L. 2020. Numerical simulation and experimental investigation of mold filling and segregation in low-pressure powder injection molding of metallic feedstock. *Advanced Powder Technology* 31(3): 1349–1358.

Tosello, G., Gava, A., Hansen, H. N. & Lucchetta, G. 2010. Study of process parameters effect on the filling phase of micro-injection moulding using weld lines as flow markers. *International Journal of Advanced Manufacturing Technology* 47(1–4): 81–97.

Tian, J., Wang, W., Shahzad, M. B., Yan, W., Shan, Y., Jiang, Z. & Yang, K. 2017. A new maraging stainless steel with excellent strength-toughness-corrosion synergy. *Materials* 10(11): 1–11.

Viswanathan, U. K., Nayar, P. K. K. & Krishnan, R. 1989. Kinetics of precipitation in 17–4 PH stainless steel. *Materials Science and Technology* 5(4): 346–349.

Wang, C. R., Xiao, H., Shao, K. W., Lu, Z. & Zhang, K. F. 2014. Densification and mechanical properties of boron carbide with micro-hole array by micro-powder injection molding. *Ceramics International* 40(6): 7915–7921.

Ye, H., Liu, X. Y. & Hong, H. 2008. Sintering of 17-4PH stainless steel feedstock for metal injection molding. *Materials Letters* 62(19): 3334–3336.

Yoo, W. Do, Lee, J. H., Youn, K. T. & Rhyim, Y. M. 2006. Study on the microstructure and mechanical properties of 17-4 PH stainless steel depending on heat treatment and aging time. *Solid State Phenomena* 118: 15–20.

Zhang, H. & German, R. M. 1992. Powder injection molding of 17-4PH stainless steel. *Proceedings of Powder Injection Molding Symposium*. 219–227.